

Effect of the magnetic order on the room-temperature band-gap of Mn-doped ZnO thin films

X. L. Wang, C. Y. Luan, Q. Shao, A. Pruna, C. W. Leung et al.

Citation: *Appl. Phys. Lett.* **102**, 102112 (2013); doi: 10.1063/1.4795797

View online: <http://dx.doi.org/10.1063/1.4795797>

View Table of Contents: <http://apl.aip.org/resource/1/APPLAB/v102/i10>

Published by the [AIP Publishing LLC](#).

Additional information on *Appl. Phys. Lett.*

Journal Homepage: <http://apl.aip.org/>

Journal Information: http://apl.aip.org/about/about_the_journal

Top downloads: http://apl.aip.org/features/most_downloaded

Information for Authors: <http://apl.aip.org/authors>

ADVERTISEMENT



Recirculation Pumps *with Speed Control*

Laser Cooling / Chillers
Brushless DC • Magnetic Drive

www.GRIpumps.com/Integrity

GRI PUMPS
A GORMAN-RUPP COMPANY

Effect of the magnetic order on the room-temperature band-gap of Mn-doped ZnO thin films

X. L. Wang,¹ C. Y. Luan,^{1,2} Q. Shao,¹ A. Pruna,¹ C. W. Leung,³ R. Lortz,⁴ J. A. Zapien,^{1,2} and A. Ruotolo^{1,a)}

¹*Department of Physics and Materials Science and Centre for Functional Photonics (CFP), City University of Hong Kong, Kowloon, Hong Kong SAR, China*

²*Center of Super-Diamond and Advanced Films (COSDAF), City University of Hong Kong, Kowloon, Hong Kong SAR, China*

³*Department of Applied Physics and Materials Research Centre, Hong Kong Polytechnic University, Hung Hom, Kowloon, Hong Kong SAR, China*

⁴*Department of Physics, Hong Kong University of Science and Technology, Clear Water Bay, Hong Kong SAR, China*

(Received 28 January 2013; accepted 6 March 2013; published online 15 March 2013)

Exchange interaction between localized magnetic moments mediated by free charge carriers is responsible for a non-monotonic dependence of the low-temperature energy band-gap in dilute magnetic semiconductors. We found that in weakly doped Mn-ZnO films, increasing the exchange interaction by increasing the concentration of free charge carriers results in a red-shift of the near-band-edge emission peak at room temperature. An increase of Mn concentration widens the band gap, and a blue-shift prevails. Exchange interaction can be used to tune the room-temperature optical properties of the wide-band gap semiconductor ZnO. © 2013 American Institute of Physics. [<http://dx.doi.org/10.1063/1.4795797>]

The wide band-gap semiconductor zinc oxide (ZnO) is commonly used in optics applications. The observation of ferromagnetism in un-doped ZnO¹ has opened up the possibility to use this compound in magneto-optics and magneto-electronics. Yet, the saturation moment at room temperature in un-doped ZnO is only a few emu/cm³, too small to be of practical use. The magnetic moment can be dramatically increased by doping with transition metals. Of particular interest is the compound Manganese (Mn)-ZnO. Mn is an iso-valent impurity for Zn, and the Mn²⁺ ionic radius (0.066 nm) is comparable to that of Zn²⁺ (0.060 nm), which assures a theoretical solubility limit of 35% (Ref. 2) while maintaining the wurtzite structure. Mn and its oxides are magnetic materials; therefore, the concern was raised³ that the observed room-temperature ferromagnetism in this compound⁴ could be due to the stabilization of an oxygen-deficient Mn_xO_y secondary phase. Theoretical and experimental studies^{5,6} have later confirmed that ferromagnetism in Mn-ZnO is genuine and must be due to an exchange interaction between magnetic moments localized at the Mn sites mediated by free charge carriers.

The magnetic moment usually increases with the increase of the concentration of oxygen vacancies because they are double donors for ZnO. Surprisingly, reports on ferromagnetism in these systems usually lack an estimation of the concentration of oxygen vacancies. The magnetic moment of doped ZnO can actually be maximized by tuning the concentration of oxygen vacancies as well as that of the dopant.

Doping with transition metals can also be used to tune the optical behavior of ZnO. In particular, doping with Mn is expected⁷⁻⁹ to widen the band gap and produce a blue-shift

in the near band edge emission peak. Interestingly, a red-shift has been reported in weakly doped Mn-ZnO nanorods^{10,11} and crystallites¹² showing ferromagnetism at room temperature. It has been therefore suggested that similarly to the case of II-VI binary dilute magnetic semiconductors,¹³⁻¹⁵ the red-shift is due to the same long-range exchange interaction which is at the origin of the magnetic order, i.e., a correlation exists in these systems between optical and magnetic properties.

We here show that a strong correlation between the magnetic and optical behavior of Mn-doped ZnO exists at room temperature in thin films with enhanced exchange interaction. In films with low concentration of Mn dopant, increasing the exchange interaction by increasing the concentration of charge carriers results in a red-shift of the near-band-edge emission peak. The expected blue-shift is recovered upon increasing the concentration of the dopant.

We fabricated three targets, respectively, pure ZnO, 2% and 4% Mn-doped ZnO, by solid state reaction method from ZnO and MnO₂ powders according to the desired stoichiometry. The powders were mixed, grounded by ball milling for 10 h, pressed to pellets, sintered at 400 °C for 8 h and then at 600 °C for 12 h. This process is to avoid the formation of high concentration clusters of Mn.³ Extensive analyses of the stoichiometry of the targets were carried out by Energy Dispersive Spectroscopy (EDS). The measurements confirmed that the stoichiometry was the expected one and uniform over each target.

Thin films were grown on Al₂O₃ (0001) crystal substrates by using a pulsed KrF excimer laser ($\lambda = 248$ nm) with a repetition rate of 10 Hz and energy 300 mJ. In order to obtain films with high concentration of oxygen vacancies we grew all the films in high vacuum (10⁻⁵ mbar). For each target we grew two sets of films. A first set of films was grown

^{a)} Author to whom correspondence should be addressed. Electronic mail: aruotolo@cityu.edu.hk

TABLE I. Properties of the grown films.

		FWHM (°)/grain size (nm)	Resistivity ($\Omega \text{ cm}^{-1}$)	Carrier concentration (cm^{-3})	M_S at RT (emu cm^{-3})
ZnO	Grown at RT	0.254/374	4.82×10^{-3}	7.14×10^{19}	0.24
	Grown at 600 °C	0.230/413	8.20×10^{-4}	6.69×10^{20}	0.64
	Grown at RT and post-annealed	0.240/400	$\sim 10^3$	$\sim 10^{12}$	0.01
2%-Mn doped ZnO	Grown at RT	0.300/317	2.12×10^{-3}	3.03×10^{20}	1.48
	Grown at 600 °C	0.240/400	6.24×10^{-4}	2.34×10^{21}	3.72
	Grown at RT and post-annealed	0.280/341	$\sim 10^3$	$\sim 10^{12}$	0.38
4%-Mn doped ZnO	Grown at RT	0.290/329	7.29×10^{-3}	1.17×10^{20}	7.52
	Grown at 600 °C	0.225/424	1.31×10^{-3}	1.01×10^{21}	12.29
	Grown at RT and post-annealed	0.247/386	$\sim 10^3$	$\sim 10^{12}$	4.31

with the substrate kept at room temperature (RT) and a second set with the substrate kept at 600 °C. As will be shown later, increasing the substrate temperature increases the concentration of oxygen vacancies. In order to compare the magnetic moment of the films with that of films having low concentration of oxygen vacancies, some of the films grown at RT were post-annealed in oxygen atmosphere at 600 °C for 3 h. Annealing in oxygen strongly suppresses oxygen vacancies. A summary of the studied films is given in Table I.

Fig. 1 shows the typical X-ray diffraction pattern of our films (for details see Table I). Only the diffraction peaks (002) and (004) from the ZnO wurtzite structure could be detected, thus confirming texturization of all the films along the *c* direction. No characteristic peak was observed for secondary Mn_xO_y phases,¹ hence confirming the formation of the solid solution $\text{Zn}_{1-x}\text{Mn}_x\text{O}$. The peak position does not significantly change upon doping with Mn. This is consistent with Vegard's law since the Mn^{2+} ionic radius (0.066 nm) is comparable to that of Zn^{2+} (0.060 nm), and the concentration of Mn in our films is much smaller than the solubility limit.² The sizes of the crystal grains are reported in Table I. They were estimated from the Full-Width Half-Maximum (FWHM) by using the Debye-Scherrer formula.

The films grown at high temperature have the best crystallinity, regardless the target used. Post-annealing leads to similar crystallographic quality but, as will be shown later, completely different electrical, magnetic, and optical properties. It is important to notice that undoped and Mn-doped

ZnO films grown under the same conditions have similar grain sizes, thus further confirming substitution of Mn^{2+} ions for Zn^{2+} ions in the ZnO matrix.

The surface morphology was studied by Atomic Force Microscope (AFM). All the as-grown films showed an average roughness $1 < R_a < 3$ nm in films of thickness ~ 500 nm (see the inset of Fig. 1). Post-annealing increases surface roughness to up to 10 nm.

The carrier concentration at room temperature, as measured by Hall measurements, does not significantly increase with doping, which excludes a significant presence of Mn in valence states other than 2+. While growing at high temperature increases the carrier concentration of about one order of magnitude in undoped, 2% and 4% Mn-doped ZnO (see Table I), post-annealing reduces the carrier concentration to below the detection limit of our Hall system. In order to estimate the resistivity and the carrier concentration in the annealed films, we had to resort to a current-perpendicular-to-plane configuration. We grew films on conductive substrates (heavily doped Niobium Strontium Titanate) and deposited a thick platinum top electrode after annealing. From the linear current-voltage characteristic of the sandwich we estimated a resistivity as large as $\sim 10^3 \Omega \text{ cm}^{-1}$ and carrier concentration as small as $\sim 10^{12} \text{ cm}^{-3}$ for undoped, 2% and 4% Mn-doped ZnO.

An *n*-type carrier concentration larger than 10^{19} cm^{-3} in the films grown in vacuum suggests that the dominant carriers are oxygen vacancies, which are double donors for ZnO. Increasing the temperature of the substrate during growth increases further the concentration of oxygen vacancies and hence the conductivity. On the contrary, the conductivity falls sharply when oxygen vacancies are removed by annealing. We can conclude that the estimation of the carrier concentration in the films grown in vacuum and not post-annealed is *de facto* an estimation of the concentration of oxygen vacancies, which are by far the dominant carriers.

Fig. 2 shows the magnetization versus magnetic field (*M*-*H*) of all the films at room temperature, as measured by using a Superconducting Quantum Interference Device (SQUID) and after subtracting the measured contribute of the substrate. For selected films we measured the magnetization versus temperature (*M*-*T*) by following a typical zero field-cooled/field cooled (ZFC/FC) protocol (not shown). The two curves could fairly be overlapped in a large range of

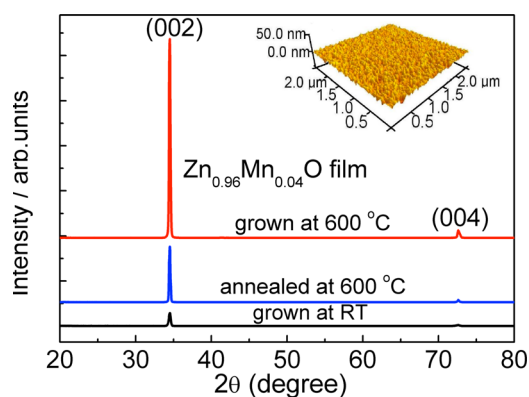


FIG. 1. XRD patterns of $\text{Zn}_{0.96}\text{Mn}_{0.04}\text{O}$ films. The inset shows the AFM scan of the as-grown film.

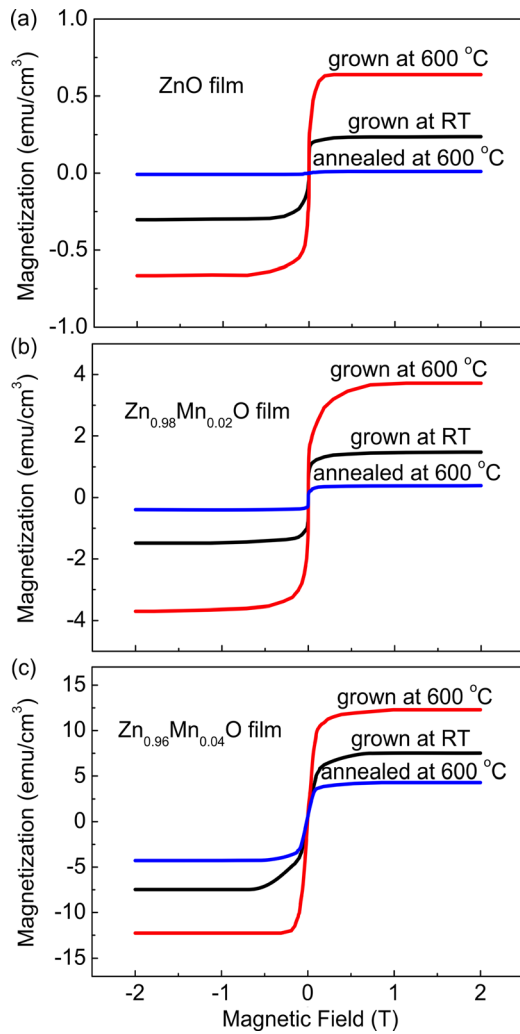


FIG. 2. M vs H curves at room temperature of (a) pure ZnO films, (b) $\text{Zn}_{0.98}\text{Mn}_{0.02}\text{O}$ films, and (c) $\text{Zn}_{0.96}\text{Mn}_{0.04}\text{O}$ films.

temperatures, hence excluding the presence of a superparamagnetic or an antiferromagnetic phase¹⁶ in our films. All the Mn-doped ZnO films show room temperature ferromagnetic order. The magnetic moment increases both with the concentration of oxygen vacancies (the mediators) and the concentration of Mn (the spin carriers). Although annealing leads to a better crystallographic quality, the magnetic moment of the annealed films decreases as compared to the as-grown films at room temperature. Clearly, the magnetic moment is related to the concentration of oxygen vacancies (M_S increases with increasing carrier concentration) and not to the crystallographic order.

It is interesting to note that a magnetic order can exist in undoped ZnO (Fig. 3(a)) films with high concentration of oxygen vacancies. Other authors¹ have ascribed this magnetic order to common superexchange coupling between oxygen vacancies, possibly organized in clusters. The strong increase in magnetic moment upon incorporation of Mn in films with the same concentration of oxygen vacancies let us confirm⁵ that ferromagnetism Mn-doped ZnO must be due to exchange between Mn cations mediated by shallow donor electrons.

Fig. 3 shows the room temperature photoluminescence spectra (PL) of the as-grown films. Being concerned with the correlation between the magnetic order and the band-gap of the films, we considered the range of wavelengths between 300 and 500 nm and normalized to the maximum intensity.

Since PL measurements are strongly affected by the surface quality of the samples under investigation, the intensity of the PL peaks of the annealed films were much smaller and the broadness larger; therefore, we limit our analyses to the as-grown films. The post-annealed films are here of interest in order to appreciate the enhancement of the magnetic moment due to oxygen vacancies and its effect on the band-gap.

The near-band-edge emission peak of ZnO is theoretically expected to be at 376 nm ($E_g(\text{ZnO}) = 3.3$ eV) and to shift to shorter wavelengths (blue-shift) when doping with Mn. This is because the band gap of MnO is larger than that of the ZnO ($E_g(\text{MnO}) = 4.2$ eV).^{7,8} The blue-shift we observe in 4% Mn-doped ZnO is in agreement with theory and with other experimental works.^{2,9}

Interestingly we observe a shift to longer wavelengths (red-shift) in 2% Mn-doped ZnO. This behavior is similar to that reported at low temperature for other dilute magnetic semiconductors, such as $\text{Cd}_{1-x}\text{Zn}_y\text{Mn}_x\text{Te}$ (Refs. 13 and 14) and $\text{Zn}_{1-x}\text{Mn}_x\text{Se}$.¹⁵ An unexpected red-shift has been reported in weakly Mn-doped ZnO nanorods^{10,11} and crystallites¹² showing ferromagnetism at room temperature. In all these works there are strong evidences of an effect of the magnetic order on the energy gap. The decrease of the band-gap is attributed to the $sp-d$ interaction between free charge carriers in the band of the semiconductor and the localized magnetic moments. The effect has been theoretically modeled by using a second order perturbation theory.¹⁵ On the other hand, ferromagnetism in Mn-ZnO is commonly believed to be due to interaction between the localized magnetic moments mediated by the free charge carriers. It is therefore reasonable to expect that an increase of the charge

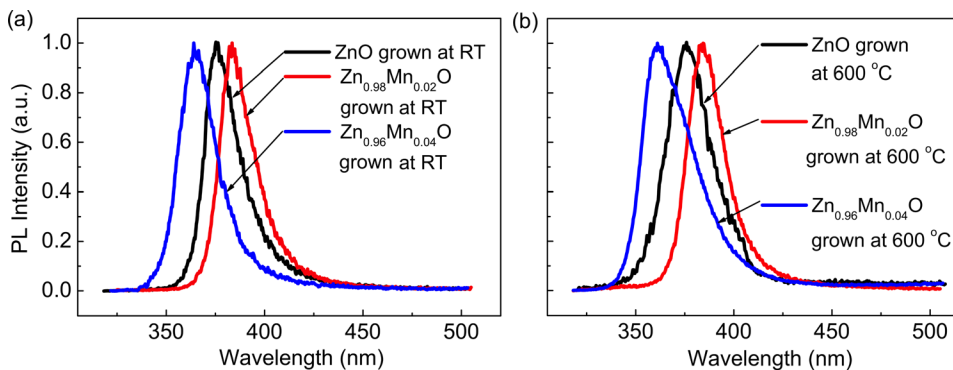


FIG. 3. Photoluminescence spectra of pure ZnO, $\text{Zn}_{0.98}\text{Mn}_{0.02}\text{O}$, and $\text{Zn}_{0.96}\text{Mn}_{0.04}\text{O}$ films grown at (a) room temperature and (b) 600 °C. The peak intensity is normalized to unity.

carriers should lead to an increase of magnetic moment and, consequently, an increase of the red-shift in the near band edge emission peak. In Figs. 2(a) and 2(b) the red-shift is, respectively, $\Delta\lambda_{RT} = 8.0$ nm and $\Delta\lambda_{600^\circ\text{C}} = 10.4$ nm with a peak position for the ZnO at $\lambda_{\text{ZnO}} = 376.4$ nm, independent on the growth temperature. This is in agreement with the increase of carrier concentration and magnetic moment in 2% Mn-doped ZnO when increasing the growth temperature (see Table I).

In conclusion, high quality undoped ZnO, 2% and 4% Mn-doped ZnO thin films were grown on sapphire by pulsed laser deposition under different conditions. Films with similar degree of crystallinity but different concentration of oxygen vacancies were investigated. We observe a red-shift at room temperature in the near-band-edge emission peak in films with 2% Mn doping. Increasing the magnetic moment by increasing the carrier concentration leads to an increase of the red-shift. Instead, increasing the Mn concentration widens the band gap, and the expected blue-shift is recovered. The red-shift is due to *sp-d* interaction between free charge carriers in the band of the semiconductor and the localized magnetic moments.

The work described in this paper was supported by the Research Grants Council of the Hong Kong Special Administrative Region, China [Projects Nos. CityU102711, CityU 104512, and SEG_HKUST03].

- ¹S. Banerjee, M. Mandal, N. Gayathri, and M. Sardar, *Appl. Phys. Lett.* **91**, 182501 (2007).
- ²T. Fukumura, Z. Jin, A. Ohtomo, H. Koinuma, and M. Kawasaki, *Appl. Phys. Lett.* **75**, 3366 (1999).
- ³P. Sharma, A. Gupta, K. Rao, F. J. Owens, R. Sharma, R. Ahuja, J. M. OGuillen, B. Johansson, and G. A. Gehring, *Nat. Mater.* **2**, 673 (2003).
- ⁴D. C. Kundaliya, S. B. Ogale, S. E. Loand, S. Dhar, C. J. Metting, S. R. Shinde, Z. Ma, B. Varughese, K. Ramanujachary, L. Salamanca-Riba, and T. Venkatesan, *Nat. Mater.* **3**, 709 (2004).
- ⁵M. Venkatesan, C. B. Fitzgerald, and J. M. D. Coey, *Nature (London)* **430**, 630 (2004).
- ⁶J. M. D. Coey, M. Venkatesan, and C. B. Fitzgerald, *Nat. Mater.* **4**, 173 (2005).
- ⁷R. Viswanatha, S. Sapra, S. S. Gupta, B. Satpati, P. V. Satyam, B. N. Dev, and D. D. Sarma, *J. Phys. Chem. B* **108**, 6303 (2004).
- ⁸Y. S. Wang, P. J. Thomas, and P. O'Brien, *J. Phys. Chem. B* **110**, 21412 (2006).
- ⁹S. W. Jung, S.-J. An, G.-C. Yi, C. U. Jung, S.-I. Lee, and S. Cho, *Appl. Phys. Lett.* **80**, 4561 (2002).
- ¹⁰Y. Guo, X. Cao, X. Lan, C. Zhao, X. Xue, and Y. Song, *J. Phys. Chem. C* **112**, 8832 (2008).
- ¹¹J. Lia, H. Fana, X. Chenb, and Z. Cao, *Colloids Surf., A* **349**, 202 (2009).
- ¹²H. W. Zhang, E. W. Shi, Z. Z. Chen, X. C. Liu, B. Xiao, and L. X. Song, *J. Magn. Magn. Mater.* **305**, 377 (2006).
- ¹³T. Donofrio, G. Lamarche, and J. C. Woolley, *J. Appl. Phys.* **57**, 1932 (1985).
- ¹⁴J. Diouri, J. P. Lascaray, and M. El Amrani, *Phys. Rev. B* **31**, 7995 (1985).
- ¹⁵R. B. Bylsma, W. M. Becker, J. Kossut, U. Debska, and D. Yoder-Short, *Phys. Rev. B* **33**, 8207 (1986).
- ¹⁶T. Fukumura, Z. Jin, M. Kawasaki, T. Shono, T. Hasegawa, S. Koshihara, and H. Koinuma, *Appl. Phys. Lett.* **78**, 958 (2001).